RSC Advances


Volume 1 | Number 1 | Jan 2013 | Pages 1–100

RSC Advances

www.rsc.org/advances

ROYAL SOCIETY
OF CHEMISTRY

www.rsc.org/advances

GRAPHICAL ABSTRACT

Sol-gel synthesis of highly pure α-Al_2O_3 nano-rods from a new class of precursors of salicylaldehyde-modified aluminum(III) isopropoxide. Crystal and molecular structure of [$Al(OC_6H_4CHO)_3$]

Anita Raj Sanwaria[a], Meena Nagar[a], Rakesh Bohra[a] *, Archana Chaudhary [b], Shaikh M. Mobin [b] , Pradeep Mathur[b] and Banwari L. Choudhary[c]

[a]*Department of Chemistry, University of Rajasthan, Jaipur-302004, India*
[b]*Discipline of Chemistry, School of Basic Sciences, Indian Institute of Technology Indore, Khandwa Road, Indore 452017, India*
[c] *USIC, University of Rajasthan, Jaipur-302004, India*
E-mail: rkbohra@sifymail.com

- Synthesis and characterization of salicylaldehyde-modified aluminum (III) isopropoxide, **[**$(OPr^i)_{3-n}Al(OC_6H_4CHO)_n$] .
- TGA, DSC of the precursors including XRD, SEM and EDX analyses of [$Al(OC_6H_4CHO)_3$] were also presented.
- Crystal and molecular structure of [$Al(OC_6H_4CHO)_3$] was discused .
- Sol-gel synthesis of α-Al_2O_3 from the precursors and $Al(OPr^i)_3$.
- The XRD, SEM, EDX, TEM, and FT-IR spectral studies of α-Al_2O_3 were also discused.

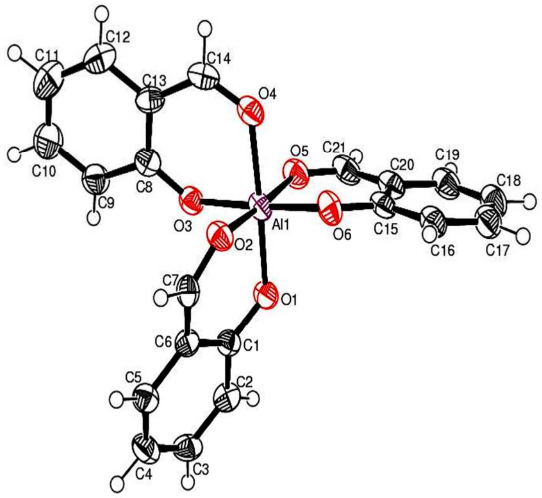

Sol-gel synthesis of highly pure α-Al_2O_3 nano-rods from a new class of precursors of salicylaldehyde-modified aluminum(III) isopropoxide. Crystal and molecular structure of [$Al(OC_6H_4CHO)_3$]

Anita Raj Sanwaria[a], Meena Nagar[a], Rakesh Bohra[a] *, Archana Chaudhary [b], Shaikh M. Mobin [b], Pradeep Mathur[b] and Banwari L. Choudhary[c]

[a]*Department of Chemistry, University of Rajasthan, Jaipur-302004, India*
[b]*Discipline of Chemistry, School of Basic Sciences, Indian Institute of Technology Indore,*
Khandwa Road, Indore 452017, India
[c] *USIC, University of Rajasthan, Jaipur-302004, India*
E-mail: rkbohra@sifymail.com

Abstract

Reactions of aluminum isopropoxide with salicylaldehyde in 1:1, 1:2 and 1:3 molar ratios in anhydrous benzene yield complexes of the type **[**(OPr^i)$_{3-n}$Al(OC_6H_4CHO)$_n$] {where n = 1(**1**); n= 2 (**2**); n= 3 (**3**)}. All the products are yellow solids and are soluble in common organic solvents. They were characterized by elemental analyses, ESI- mass, FT-IR and (^{1}H, ^{13}C& ^{27}Al) NMR studies. The ESI-mass spectral studies indicate dimeric nature for **(1) & (2)** and monomeric nature for the compound **(3)**. Crystal and molecular structure of [$Al(OC_6H_4CHO)_3$]**(3)** suggest that salicylaldehyde ligands bind the metal in a side on dihapto η^2-(O,O) manner, leading to the formation of an hexa- coordinated environment around the aluminum atom. The powder XRD, SEM image, and EDX analysis appear to indicate formation of nano-sized rods for the precursor **(3)**. Sol-gel hydrolysis of all the precursors Al(OPr^i)$_3$, **(1), (2) & (3)** followed by sintering at 1100° C yielded α- Al_2O_3 **(a), (b)**, **(c)** and **(d)** respectively. The powder X-ray diffraction patterns and the SEM images of all the oxides exhibit nano-sized microcrystalline morphology for **(a)** and mixed platelike nano-rods morphology for **(b), (c)** and **(d)** . The EDX and TEM studies of **(d)** also corroborate the formation of α- Al_2O_3. The IR spectral studies of all the oxides indicate the formation of pure α-alumina, a versatile ceramic oxide known for exhibiting a wide variety of applications in engineering and biomedical areas.

Keywords: Nano-sized α- alumina. Nano-rods. Molecular structure of [$Al(OC_6H_4CHO)_3$]. Sol-gel precursors for Al_2O_3.

1. Introduction

Corundum (α-Al_2O_3) is one of most important ceramic materials due to its high strength at elevated temperatures, hardness, high-melting point, thermal conductivity, chemical inertness, large band-gap, abrasion resistance and thermal shock resistance properties[1-7]. Such excellent properties made it the best quality ceramic material for a wide range of applications in engineering (electronics; optoelectronics; reinforcement filler in composites; cutting tools; spark-plugs; thermo-luminescent dosimeters and uses in refractory materials) [8-15], biomedical areas (bio-ceramic materials; inert ceramic materials in medicine and dentistry) [16,17] as well as in modern surgery (total artificial hip replacement; knee joint implants and bone screws) [18, 19].

Alpha-alumina nano-structures such as nanotubes, nanowires, nanobelts, nanoplatelets, spherical nanoparticles have been receiving increasing attentions[20-24]. Reported synthetic methods for nano-sized α-Al_2O_3 are chemical vapor deposition (CVD) [21], combustion chemical deposition (CCD) [22], atomic layer deposition (ALD) [28], spray pyrolysis[27], solution combustion synthesis (SCS) [26], sol-gel method using different organic precursors: aluminum secondary butoxide, aluminum nitrate or aluminum isopropoxide[25, 29-31].

It would be interesting to mention here that aluminum(III) complexes of 8-hydroxyquinoline like Alq_3 have been widely used as a precursor for the fabrication of organic electroluminescent diodes[32-34]. Although formation of δ- Al_2O_3 from 8-hydroxyquinoline modified aluminum(III) isopropoxide has recently been reported[35], yet little is known about the formation of α-Al_2O_3 from chemically modified aluminum(III) alkoxide precursors[36].

Herein, we report sol-gel synthesis of highly pure α-Al_2O_3 nano-rods from a new class of salicylaldehyde –modified aluminum (III) isopropoxide precursors and crystal and molecular structure of $[Al(OC_6H_4CHO)_3]$**(3)**.

2. Results and discussion

2.1 Synthesis and characterization of aluminium(III) isopropoxide derivatives with salicylaldehyde (HOC_6H_4CHO):

Reactions of aluminum(III) isopropoxide with salicylaldehyde (HOC_6H_4CHO) in 1:1, 1:2 and 1:3 molar ratios in anhydrous benzene yield precursors of the following type :

$$Al(OPr^i)_3 + nHOC_6H_4CHO \xrightarrow[reflux(4h)]{benzene} [(CHOC_6H_4O)_nAl(OPr^i)_{3-n}] + nPr^iOH \uparrow$$

[Where n = 1**(1)**; n= 2**(2);** n= 3**(3)**]

The above reactions were quantitative and their progress was monitored by determining the liberated 2-propanol in benzene-2-propanol azeotrope by oxidimetric method[32]. All the three products **(1)**, **(2)** and **(3)** were yellow solids, soluble in common organic solvents. The products were characterized by FT-IR, (^{1}H, ^{13}C & ^{27}Al) NMR spectral studies. Synthetic and elemental analyses of all these complexes were summarized in table 1. The ESI mass spectral studies indicate dimeric nature for **(1)** and **(2)** and monomeric nature for **(3)** (Table-2)

2.1.1 IR and NMR spectra

The IR and (^{1}H &^{13}C) NMR spectral data of all these derivatives are summarized in table 3.

In IR-spectra broad stretching vibrations at ~3145 cm^{-1} due to OH group of the free ligand disappeared, suggesting the deprotonation of –OH group and concomitant formation of Al-O bond[35,37]. Bands in the region 643-645 cm^{-1} may be assigned to ν (Al-O) stretching vibrations [33,34].The medium intensity band observed in the region of 1000-1003 cm^{-1} is assigned to ν(C-O) of the isopropoxy group. The Al-O-Al vibrations have been observed in the region 755-756 cm^{-1} [38-40]. The IR spectrum of the salicylaldehyde ligand exhibits an aldehydic ν(C-O) stretching band at about 1670 cm^{-1}, which undergoes a downfield shift in the precursors **(1)**, **(2)** and **(3)** at ~ 1660, 1650 & 1640 cm^{-1}, respectively, indicating coordination of the aldehydic group with the aluminum atoms in the precursors.

In the ^{1}H NMR spectra, the signal due to hydroxyl proton of the free ligand at (8.80 ppm) are found to be absent in all these derivatives, suggesting the formation of Al-O bond by deprotonation of the –OH group of the free ligand. The methine protons of the bridging and terminal isopropoxy groups overlapped to give a multiplate in the range 4.0-4.29 ppm. Similarly, the methyl protons of the bridging isopropoxy groups appear at 1.11-1.37 ppm as broad doublets and the terminal isopropoxy groups appear at 1.46-1.48 ppm, also as doublets with different intensities, indicating the nonequivalent nature of the bridging and terminal isopropoxy groups in **(1)** and **(2)**.

In the ^{13}C NMR spectra of all the complexes the distribution of new resonance lines (114.14-195.01 ppm) of ligand moiety indicate bonding between aluminium(III) and salicaldehyde. The characteristic chemical shifts values of the isopropoxy groups in were at 25.31-27.95 ppm and 63.05-66.07 ppm assignable to methyl and methine carbons, respectively. Similarly, two signals each for methyl and methine carbons of the bridging and terminal isopropoxy groups were observed in compounds **(1)** and **(2)** suggesting the nonequivalent nature of the isopropoxy groups in these derivatives.

The ^{27}Al NMR spectrum of **(1)** [Fig.1A] at room temperature exhibits broad signals at ~75.55 ppm, indicating the presence of tetra-coordination around aluminum(III) atoms[39-42] exist in solution. The ^{27}Al NMR spectrum of **(2)** [Fig.1B] exhibits two signals at ~3.5 and at ~70.99 ppm, indicating the presence of both hexa- and tetra-coordinated aluminum atoms exist in solution. In the absence of a single crystal X-ray diffraction study, it is not possible to comment on the exact molecular structure of such derivatives, yet the above studies do suggest the possibility of an binuclear structure containing four -coordination around both aluminum(III) atoms in **(1)** [Fig.2(I)] and binuclear structure containing six- and four -coordination around aluminum(III) atoms in **(2)** [Fig.2(II)] and The ^{27}Al NMR spectrum of **(3)** [Fig-1C] exhibits signal at ~3.88 ppm, indicating that six –coordination around aluminum species is present in solution [Fig.2 (III)].

2.1.2 Single crystal X-ray analyses of [Al $(OC_6H_4CHO)_3$] (3)

The precursor **(3)** is monoclinic and crystallizes in space group P $2_1/n$. The three salicylaldehyde ligands bind the metal in dihapto η^2-(O, O) manner leading to the formation of a hexa-coordinated environment around the aluminum atom. The selected bond lengths and bond angles are summarized in table-4. The Al–O bond lengths are varying between 1.841 Å and 1.914Å. The *cis* O–Al–O angles range from 87.39° to 94.53° while the *trans* O–Al–O angles vary from 176.10(11)° to177.73(10)° , indicating that the aluminum atom in the complex occurs in a distorted octahedral environment. The structure indicates that AlO_6 core is constructed from six oxygen atoms of three salicylaldehyde ligands (Fig.3). Aluminum content was found to be 10% from the chemical analysis of **(3)**. The metal content is in agreement with the calculated value of 10.1% for the above structure. Considering the structure and aluminum content, formula can be fixed as $[Al(OC_6H_4CHO)_3]$ and the crystal and molecular structure is shown in fig.3 .

A comparison with the known corresponding crystal structures of Al(acac)$_3$ and Alq$_3$ (where acacH = acetylacetone and qH = 8-hydroxyquinoline)[43,44] do suggest that all the bond lengths and bond angles are in the expected range.

2.1.3 XRD, SEM and EDX of [Al(OC$_6$H$_4$CHO)$_3$](3)

The X-ray powder diffraction spectrum of the precursor **(3)** dried at 100°C is shown in fig. 4, exhibits crystalline nature of the product. In the X-ray powder diffraction spectrum, the dominant peaks are at 2θ = 11.12^o, 12.79 ^{o}, 14.18^o, 17.62 ^{o}, 20.22^o, 23.08^o, 25.39^o, 26.93^o, 30.24^o, 34.01^o,35.94^o, 38.70^o, 40.37^o, 42.62^o,45.14^o and 46.65^o. Their calculated inter-planar distances are 7.94, 6.91, 6.23, 5.02, 4.38, 3.84, 3.49, 3.30, 2.95, 2.63, 2.49, 2.32, 2.23, 2.11, 2.00 and 1.94 , corresponds to diffraction from (101), (012), (003), (020), (120), (122), (-115), (030), (-224) , (231), (040), (-403), (-333), (-415), (-219), and (-407) planes, respectively. The average particle size (~ 40 nm) was calculated, using the *Debye Scherrer equation*[45] from the major reflections {(012), (020), (120), (122)}. The SEM image of **(3)** indicates formation of nano-sized rods like morphology and EDX analysis [Fig. 4] corroborates the molecular formula [Al(OC$_6$H$_4$CHO)$_3$].

2.1.4 TGA & DSC curves of the precursors (1-3)

Thermogravimetric and DSC curves of the precursors **(1-3)** are shown in fig. 5. It appears that the precursors **(1)** and **(2)** are thermally less stable as compared to **(3)**. The onset decomposition begins at different temperatures for all the precursors **(1-3)** indicating different degrees of thermal stability. TGA curves show multistep decomposition in all the complexes. Appearance of multiple weight loss stepes in the curves of all the three derivatives, indicate multiple thermal events due to organic pyrolysis under nitrogen atmosphere and the decomposition appears to be almost completed at about 900^{o}C. Formation of pure Al$_2$O$_3$ does not appear to be the final product. The DSC curves show that the decomposition reaction is exothermic at ~500°C and endothermic at ~650^{o}C & 800°C.

2.2 Hydrolytic studies of (1-3) by the sol-gel technique

Schematic representation of the hydrolytic process of Al(OPr^i)$_3$, **(1), (2)** or **(3)** are shown as fig. 6:-

In order to control the size of the desired material, initially the precursors were subjected to small hydrolysis ratio (one drop of a miture of 1 mL water and 4 mL anhydrous 2-propanol) during stirring[46]. Finally, excess water was added after small intervals (6–8 h) and stirred for 2 days. Thus, the hydrolysis of the precursors $Al(OPr^i)_3$ and **(1-3)** followed by sintering at 1100°C for 2 h afford formation of alumina (a) from $Al(OPr^i)_3$, (b) from **(1)**, (c) from **(2)** and (d) from **(3)**.

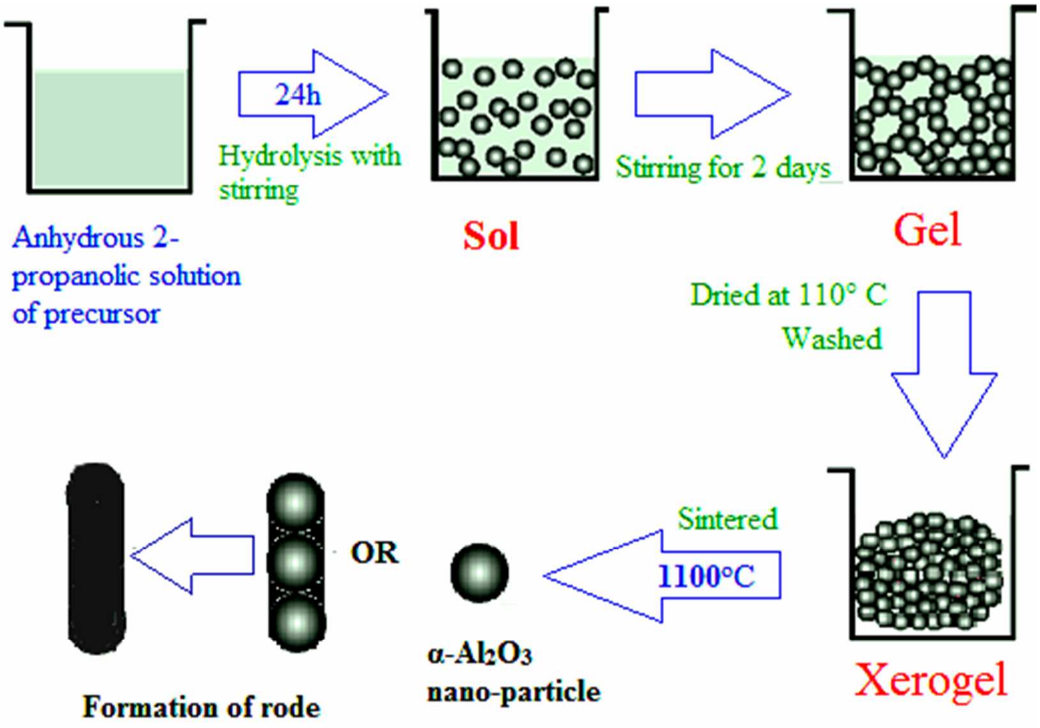

Fig 6. Proposed mechanism for the formation of α-Al_2O_3 nano-particle/rode.

2.3 Material characterization

The XRD analysis showed the most stable phase, α -Al_2O_3 occurred dominantly in all the oxides at 1100°C. These were characterized by FT-IR, XRD, SEM, EDX, TEM and SAED pattern analyses.

The XRD patterns of oxides **(a)-(d)** obtained from sol-gel hydrolysis followed by sintering at 1100^0C/3h of $Al(OPr^i)_3$, **(1), (2) & (3)** respectively, are presented in fig.7. Peak positions in all oxides (α-Al_2O_3) shows at 2θ= 25.34°, 34.89°, 37.49°, 43.09°, 52.30°, 57.23°, 59.50 °, 61.05 °, 66.26 ° and 67.93° corresponds to diffraction from (012), (104), (110), (113), (024), (116), (211), (122), (214) and (300) planes. Comparisons of these patterns with the reported pattern of α -Al_2O_3 **[JCPDS # 46-1212]** have been made which suggest the formation of high purity α- alumina (hexagonal rhomb-centered phase with a = 4.758 Å, b= 4.758 Å, c = 12.99Å). The sizes of the α- Al_2O_3 obtained from the modified precursors were evaluated from *debye-scherrer equation* [45] are ~16 nm **(a)** , ~14 nm **(b)** ,~12 nm **(c)** and ~11 nm **(d)** .

Scanning electron microscopic (SEM) images of α- Al_2O_3 **(a-d)** are shown in fig. 8, indicate the nano-sized microcrystalline morphology for **(a)** and mixed platelike rods morphology for **(b), (c)** and **(d)**. Further characterization of the nanostructures was carried out using transmission electron microscopy and the selected area electron diffraction (SAED) pattern as shown in fig. 9. The TEM image of representative oxide **(d)** reveals that the nano-rods of α-Al_2O_3, size with average range of about 10-15 nm. The SAED pattern {d = 3.4 Å, corresponding plan (024)} can be indexed as hexagonal rhomb-centered of α-Al_2O_3, it is in complete agreement with XRD observation, thus it is evident that each individual α-Al_2O_3 nano-rode is a single crystal. In order to investigate the EDX and quantitative weight % results of α-Al_2O_3 **(d)** as shown in [Fig. 9] were also carried out indicating the formation of pure α -alumina.

IR absorption spectra of the α- Al_2O_3 oxides are show the large band between 750 and 400 cm^{-1} is a characteristic absorption band of transition alumina and the stable phase of α-Al_2O_3 it is attributed to stretching vibration of the Al-O-Al bond[47-49]. Significant bands at ~600, ~500 and ~450cm^{-1} emerge in the spectra, which are recognized to be the characteristic absorption bands of α- Al_2O_3[50].

3. Experimental

3.1 Materials and methods

All the experimental manipulations (except hydrolysis reactions) were carried out under strictly anhydrous conditions. Solvents and reagents were dried and purified by conventional methods and distilled/ sublimed prior to use[51]. *Due precautions were taken to handle health hazard chemicals, like benzene.* Aluminium(III) isopropoxide was synthesized and purified as reported in the literature[52]. Infrared spectra (4,000-400 cm^{-1}) were recorded as dry KBr pellets on SHIMADZU FT-IR 8400 spectrometer. The ^{1}H and ^{13}C-NMR data were collected on a JEOL FX 300 FT NMR spectrometer at 300.4 and 75.45 MHz frequencies for ^{1}H and ^{13}C NMR, respectively in a solution of $CDCl_3$ using TMS as internal standard. The ^{27}Al NMR spectral studies were carried out in $CDCl_3$ using aluminum nitrate as an external reference in aqueous solution at 100 MHz. Thermo-gravimetric analyses were performed on Metler Toledo thermal analysis system with the heating rate 0–900/10°C under a nitrogen atmosphere. ESI mass were performed on Agilent 1100 LC/MSD SL quadrupole mass spectrometer (Agilent LC/MSD API-Electrospray SL G2708DA). The XRD patterns were recorded on PANalytical make X'Pert PRO MPD diffractometer (model 3040). SEM and EDX were performed on Carl -Zeiss (30keV) make and model EVO 18. TEM was carried out on FEI Technai (200 keV) G2 S-T win. The C, H, N - analyses were performed on Thermo scientific Flash 2000.

3.2 Preparation of [Al($OC_6H_4CHO)_3$](3)

An anhydrous benzene solution of salicylaldehyde (2.97g, 24.34 mmol) was added to an anhydrous benzene solution of Al($OPr^i)_3$ (1.66g, 8.12 mmol). The contents were refluxed for ~ 4 h on a fractionating column and completion of the above reaction was monitored by estimating the liberated 2-propanol collected azeotropically with benzene. Resulting mixture was concentrated in vacuum to give a dark yellow solid (3.17g, 99.36 % yield). The other derivatives **(1)** and **(2)** were prepared by the above similar procedure.

3.3 Hydrolysis of [Al($OPr^i)_2(OC_6H_4CHO)]_2$(1)

3.2 g of the precursor **(1)** was dissolved in anhydrous 2-propanol (~30mL). To this yellow colored clear solution, a drop of a mixture of distilled water- 2-propanol (1 mL water and 4mL anhydrous 2-propanol) was initially added gelation occurred immediately. Excess of stoichiometric amount (0.43) of water was then added in small lots with continuous stirring for 4-5 h to ensure complete hydrolysis. The mixture was further stirred for 2 days at room temperature. A yellow colored gel was obtained. It was dried in a preheated oven (at >100°C), to yield a yellow powder. In order to remove the organic/inorganic impurities, the powder was washed several times with distilled water and then with a mixture of n-hexane and acetone (1:1). The resulting powder was sintered at 1100°C for 2h in a muffle furnace to give pure white colored powder, which was characterized by powder XRD as α- alumina. Hydrolyses of the other precursors Al($OPr^i)_3$, **(2)** and **(3)** were carried out by the above similar procedure.

3.4 Crystal and molecular structure of [Al($OC_6H_4CHO)_3$](3)

When 2.29 g of **(3)** was subjected to re-crystallization in a mixture of dichloromethane and n-hexane, well-shaped yellow shiny single crystals were obtained which was covered in Paratone-N and placed rapidly into the cold N_2 stream of the Cryo-Flex low temperature device.

Single crystal x-ray diffraction data were collected on an Agilent technologies supernova X-ray diffraction system. Data were collected at 150(2) K using graphite-monochromoated Mo-Kα radiation (λ_α = 0.71073 Å). The strategy for the Data collection was evaluated by using the CrysAlisPro CCD software. The data were collected by the standard 'phi-omega scan' techniques and were scaled and reduced using CrysAlisPro RED software. The structures were solved by direct methods using SHELXS-97 and refined by full matrix least squares with SHELXL-97, refining on F^2.

The positions of all the atoms were obtained by direct methods. All non-hydrogen atoms were refined anisotropically. The remaining hydrogen atoms were placed in geometrically constrained positions and refined with isotropic temperature factors, generally 1.2 x U_{eq} of their parent atoms. Molecular drawings were obtained using the program ORTEP (Fig.3). The crystal and refinement data are summarized in table 5 for $[Al(OC_6H_4CHO)_3]$**(3)**

4. Conclusions

The nano-shaped rods of the precursor $[Al(OC_6H_4CHO)_3]$**(3)** are easily formed at ~ 100°C. This observation is similar to that reported for Alq_3[34, 35], most commonly used material for OLEDs applications suggesting possibility of application of $[Al(OC_6H_4CHO)_3]$**(3)** in this direction. Highly pure α-Al_2O_3 material was obtained from salicylaldehyde modified aluminum(III) isopropoxide precursors **(1-3)** through a sol-gel method. The salicylaldehyde modification of aluminum(III) isopropoxide appears to control the particle size, shape and purity .The α- Al_2O_3 exhibit a wide verity of applications in engineering and biomedical sciences.

5. Supplementary material

Crystallographic data for $[Al(OC_6H_4CHO)_3]$ (CCDC No. 987154) has been deposited at the Cambridge Crystallographic Data Centre. These data can be obtained free of charge via http:// www.ccdc.cam.ac.uk/conts/retriving .html, or from the Cambridge Crystallographic

Data Centre, 12 Union Road, Cambridge CB2 1EZ, UK; fax: (+440 1223-336-033 or email deposit@ccdc.cam.ac.uk

Acknowledgements

We are grateful to DST and CSIR New Delhi for financial support .We are highly thankful Department of physics and USIC ,UOR for carrying out XRD, EDX ,SEM and TEM analyses and Therachem Research.medilab, Jaipur for ESI mass analyses.

Reference

1. F. S. Yen, J. L. Chang, P. C. Yu , *J.Cryst.Growth* ., 2002, **246**, 91-98.
2. P. C. Yu , F. S. Yen and T.C. Lin, *J.Cryst.Growth* ., 2004, **265** , 137-148.
3. F. S. Yen, P. L. Chang, P. C. Yu and R. Yang, *J. Eng. Mater.,* 2007, **351**, 81-87.
4. A. Jawaorek, A. T. Sobczyk, *J. Electrostatic* , 2008 , **60**, 197-102.
5. M.R. Saoubi & S.Ruppi , *CIRP Annals – Manu. Tech.,* 2009, **58**, 57–60.
6. R. Ianson, I. Lazau and C. Pacurariu , *J. Mater. Sci.,* 2009, **44** , 1016-1023.
7. M. R. Noordin, K.Y. Liew, *Book edited by Ashok Kumar*, 2010, **21**, 406-418.
8. J. Lawrence and L. Li, *J. Appl. Sur. Sci.*,2000, **168** ,71-74.
9. E. Volceanov, A. Volceanov and S. Stoleriu, *J.Eur.Ceram.Soc.,* 2007, **27,** 759-762.
10. D. Gitknecht, J. Chevalier,V. Garnier, G.Fantozzi, *J.Eur.Ceram.Soc.,* 2007, **27,** 1547-1552.
11. G. Zhang, L. Bingchao, J. Zhang and W. Cai, *Natural Sci. Mater. Int.,* , 2012, **22(2) ,** 153-159.
12. B. Vermang, P. Choulat, H. Goverde, J. Horzel, J. John, R. Mertens, and J. Poortmans, *Energy Procedia* , 2012, **27**, 325-329.
13. F. Mirjalili, L. Chuah, M. Khalid and M. Hasmaliza, *J. Thermo. Compo. Met.,* 2012, **25,** 453-467.
14. S. Lu, L. Zhang and Y. Liu, *RSC Adv.,* 2013 , **3,** 5639-5648.
15. M. H. Zadeh, M. Razavi, O. Mirzaee, R. Ghaderi, *J. King Saud Uni. Eng. Sci.,* 2013 , **25,** 75-80.
16. J. Lawrence *J. Optical and lasers in Engineering,* 2004, **41,** 505-514.
17. M.A. Shah and J. Kumar, *J. Afri. Phy. Review*, 2008, **2** ,48-51.

18. J. Li and G.W. Hasting, A Handbook of biomaterial properties. London: Chapman & Hall, 1998, 340-353.

19. A.H.D. Aza, J. Chevalier, G. Fantozzi , M. Schehl and R. Torrecillas, *Biomaterials,* 2002, **23** , 937-945.

20. Z. L. Xiao, C. Y. Han, U. Welp, H. H. Wang, W. K. Kwok, G. A. Willing, J. M. Hiller, R. E. Cook, D. J. Miller, and G. C. Crabtree, *Nano Lett.,* 2002, **2 (11)**, 1293-1297.
21. Y. Zhang, R. Li, X. Zhou, M. Cai, and X. Sun, *J. Nanomater.* , 2008, 1-8.
22. Z. Zengzhi, *Energy Procedia.,* 2012, **27,** 1284-1291.
23. H. Sadabadi, A. Aftabtalab, S. Zafarian, K. V. Rao and V. Rajendar, *J. Eng.Adv. Tech.,* 2013, **2(3)**,54-56.
24. F. Mirjalili, L. Chuah and H. Mohamad, *J.Ceramic Pro. Res.,* 2011, **2,** 738-741
25. J. A. Wang, X. Bokhimi, V. Morales, O. Novaro, T. Lopez and V. Gomez, *J.Phy.Chem*., 1999, **103,** 299-303.
26. A. M. Azad, *Mater. Sci. Eng.,* 2006, **435-436**, 468-473.
27. R.M.Laine, J.C.Marchal, H.P.Sun and X.Q.Pan, Nature Mater. 5(2006) 710-712.
28. P. Repo, H. Talvitie, S. Lib, S. Skarp, H. Savin, *Energy Procedia* (2011) 681-687.
29. H. Sadabadi, A. Aftabtalab, S. Zafarian, S. Shaker, M. Ahmadipourand and K.V.Rao1, *J. Sci. Eng. Res.,* 2013, **4** , 1593-1596.
30. P. Padmaja, P. K. Pillai and K. G. A. Warrier*, J. Porous Materials,* 2004, **11**, 147-155.
31. R. Rogojan, E. Andronescu, C. Ghitulica and B. S. Vasile , *Sci. Bull,* 2011, **73,** 68-76.
32. T. Miyamae, E. Ito, Y. Noguchi and H. Ishii, *J. Phys. Chem.,* 2011, **115,** 9551.
33. R. H. Friend, R. W. Gymer, A. B. Holmes, J. H. Burroughes, R. N. Marks, C. Taliani, D. D. C. Bradley, D. A. Dos Santos, J. E. Bredas, M. Logdlund, W. R. Salaneck, *Nature,* 1999, **397,** 121-128.
34. J.S. Hu, H.X. Ji, A.M. Cao, Z.X. Huang, Y. Zhang, L.J. Wan, A.D. Xia, D.P. Yu, X.M. Meng and S.T. Lee, *Chem.Commun.,*2007, 3083-3085.
35. A. R. Sanwaria, N. Sharma, A. Chaudhary and M. Nagar, *J. Sol-Gel Sci. Tech.,* 2013, **68**, 245-253.
36. T. Yogo and H. Iwahara, *J. Mater Sci*, 1992, **27**, 1499-1405.
37. D. C. Bradley, F. M. A. Halim and W. Wardlaw, *J. Chem. Soc.*, 1950, 3450, 3454-3454.

38. A. K. Jain , A. Gupta, R. Bohra, I. P. Lorenz and P. Mayer, *Polyhedron,* 2006, **25,** 654-662.
39. A. Dhammani, R. Bohra and R. C. Mehrotra , *Polyhedron ,* 1998, **17,** 163-169.
40. K. Thangarju, P. Amaladass, K. S. Bharathi, N. Kumar, *J. Appl. Surf. Sci.*, 2009, **255,** 5760-5763.
41. N. Sharma, R. K. Sharma, R. Bohra, J. E. Drake, M. B. Hursthouse and M. E. Light, *J. Chem.Soc. Dalton Trans*., 2002, 1631-1634.
42. N. Sharma, A. R. Sanwaria , M. Nagar and R. Bohra, *Main Group Met. Chem.*, 2013, **36,** 109-115.
43. M. Shirodker, V. Borker, C. Nather, W.Bensch and K.S. Rane , *Indian Journal of Chem.,*2010, **49**, 1607-1611.
44. N. Johansson, T. Osada, S. Stafstron, W.R. Salaneck, V. Parente, D.A. Santos, X. crispin and J.L.Bredas, *Journal of Chemical physics,* 1999, 111, 2157-2163.
45. B. E. Warren , X-ray diffraction. Dover publication, New York, p 13, 1990.
46. V.G. Kessler, *J. Sol- Gel Sci Technol,* 2009, **51,** 264–271
47. M. I. Baraton and P. Quintard, *J. Mol. Struct.,* 1982, **79,** 337-340.
48. T. M. H. Costa, M. R. Gallas, E. V. Benvenutti and J. A. H. Jornada, *J Phys. Chem.* 1999, **103,** 4278-4284.
49. L. Jiang, P. Yubai, X. Changshu, G. Qiming and Jingkun, *Ceramic International,* 2005 **32**, 587-591.
50. F. Mirjalili, L. Chuah, H. Mohamad, F. A. Razi and A. B. Dayang Radiah*, J. Ceramic Pro. Res.,* 2011, **2,** 738-741.
51. A. I. Vogel, Text Book of Quantitative Chemical Analysis. 5th edn., Longmans, London ,1989
52. D. C. Bradley, R. C. Mehrotra, I. P. Rothwell and A. Singh, Alkoxo and Aryloxo Derivatives of Metals Academic Press London (2001)

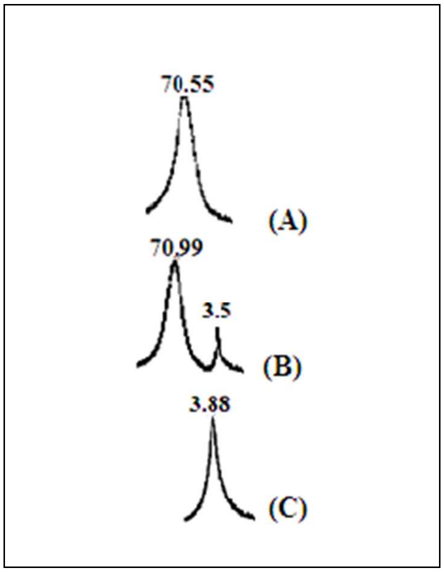

Fig: 1. A, B & C are ^{27}Al NMR spectra at room temperature of the precursors (1),(2) and (3) respectively .

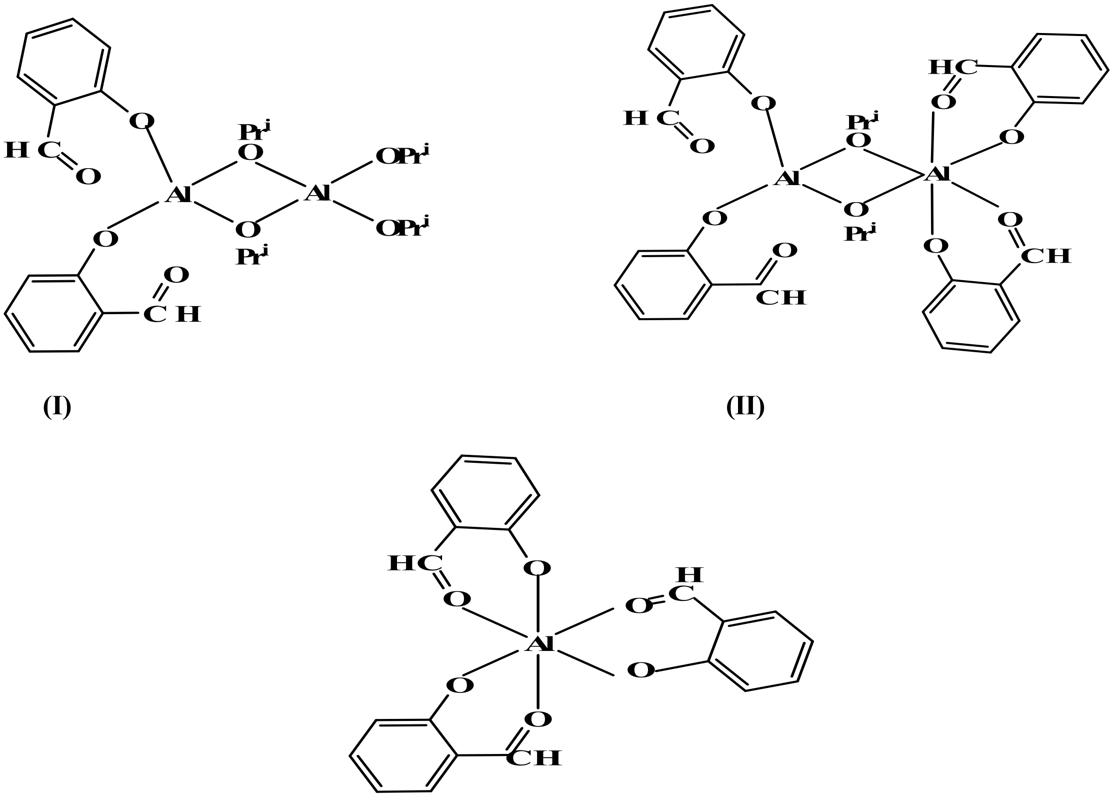

(I) **(II)**

(III)

Fig: 2. I, II & III are proposed structures of the precursors (1),(2) and (3) respectively .

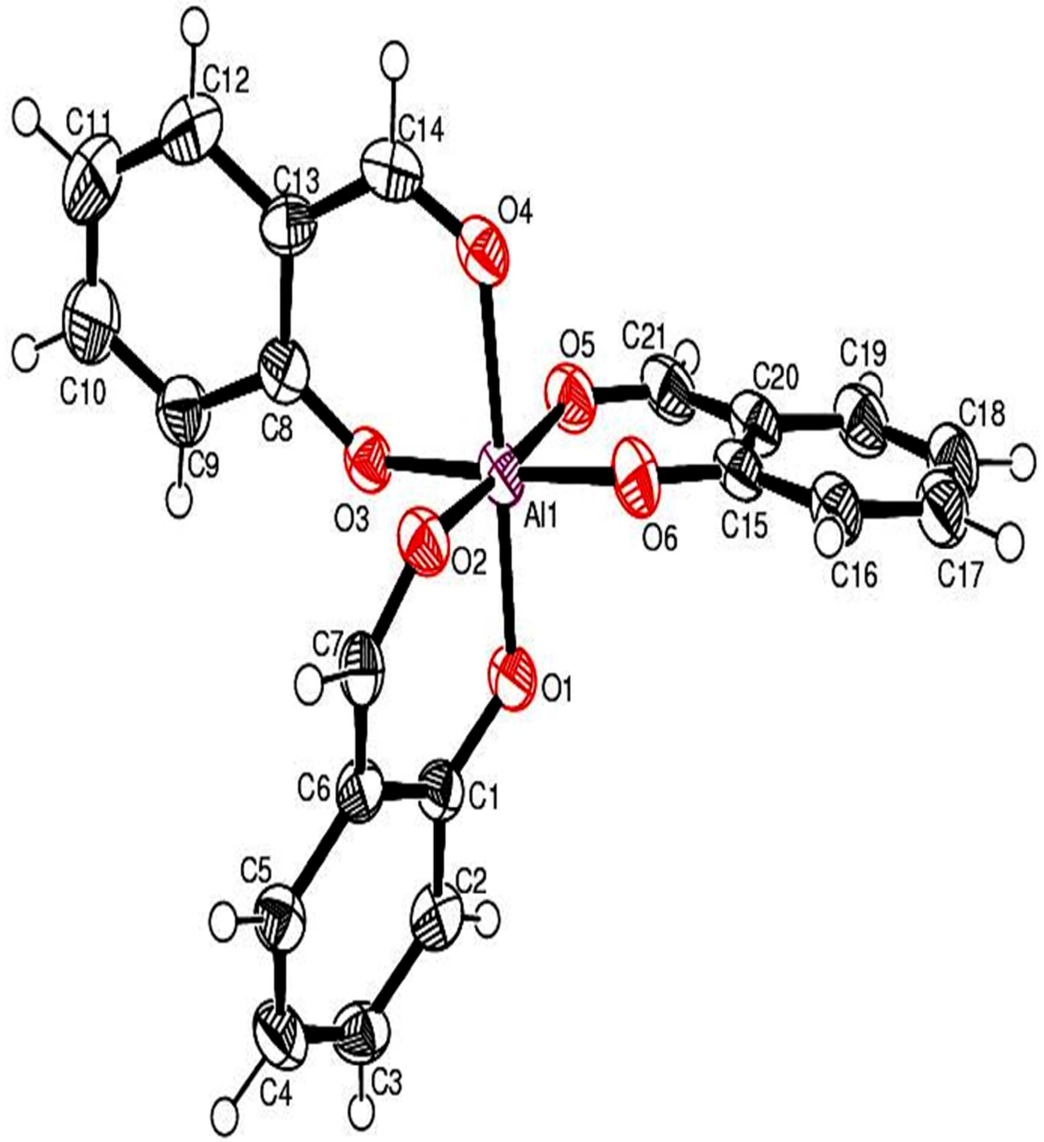

Fig. 3 Crystal structure / ORTEP plot of the molecule [Al(OC$_6$H$_4$CHO)$_3$] (3) showing the atom labeling scheme.[Displacement ellipsoids are drawn at 50% probability level , except for the H atoms which are shown as circles of arbitrary radius].

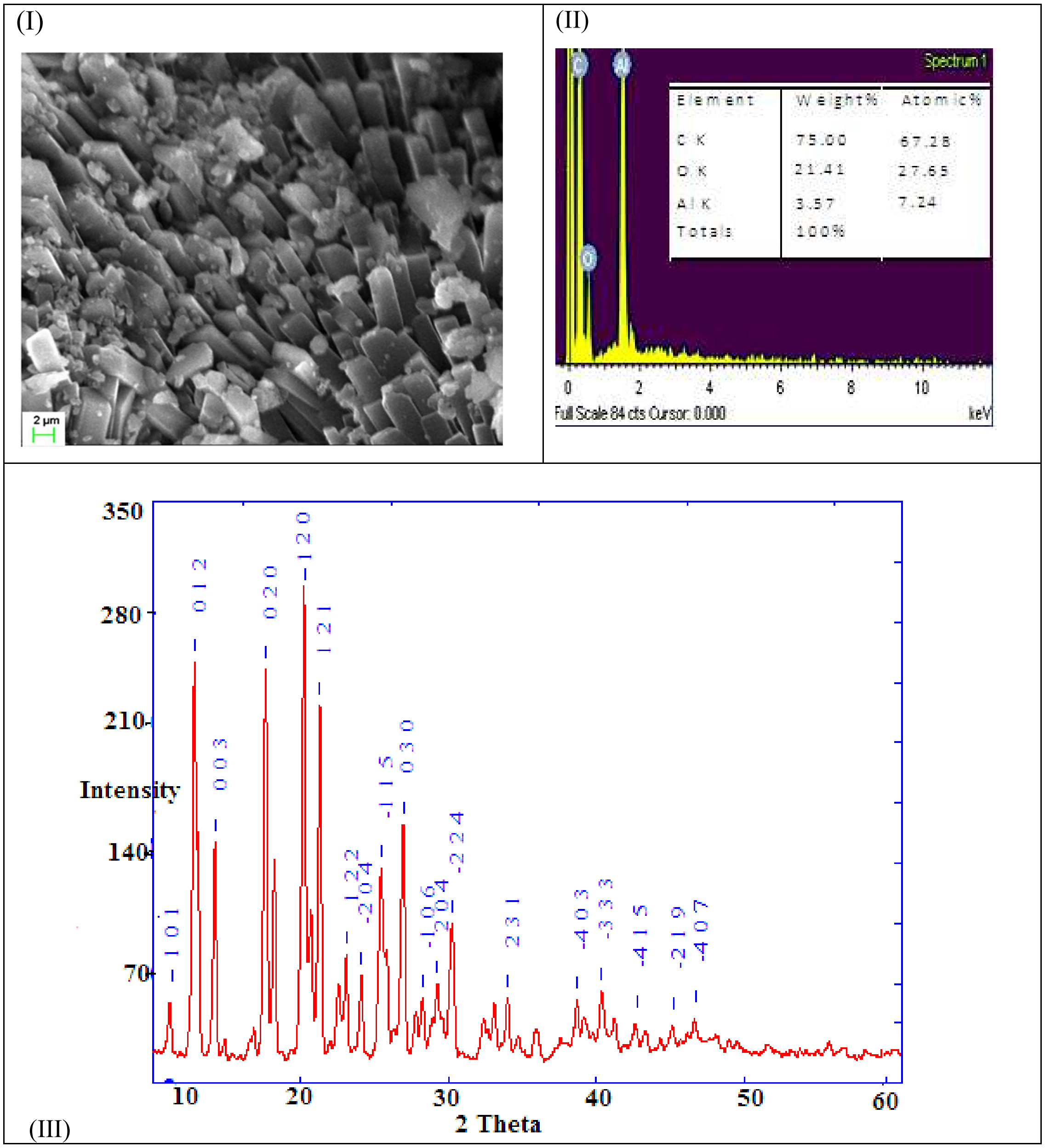

Element	Weight%	Atomic%
C K	75.00	67.28
O K	21.41	27.65
Al K	3.57	7.24
Totals	100%	

Fig. 4 (I) SEM image, (II) EDX and (III) XRD spectrum of the precursor $[Al(OC_6H_4CHO)_3]$ (3) dried at ~100°C.

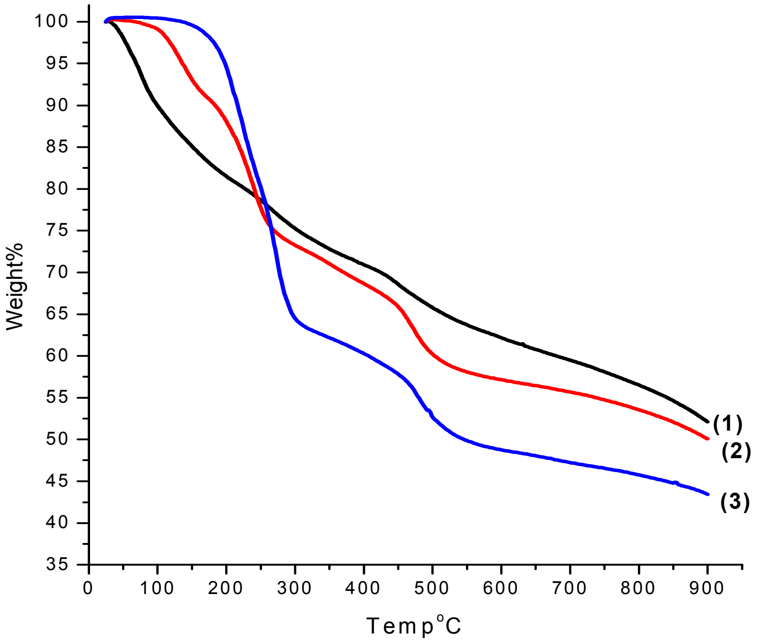

(a)

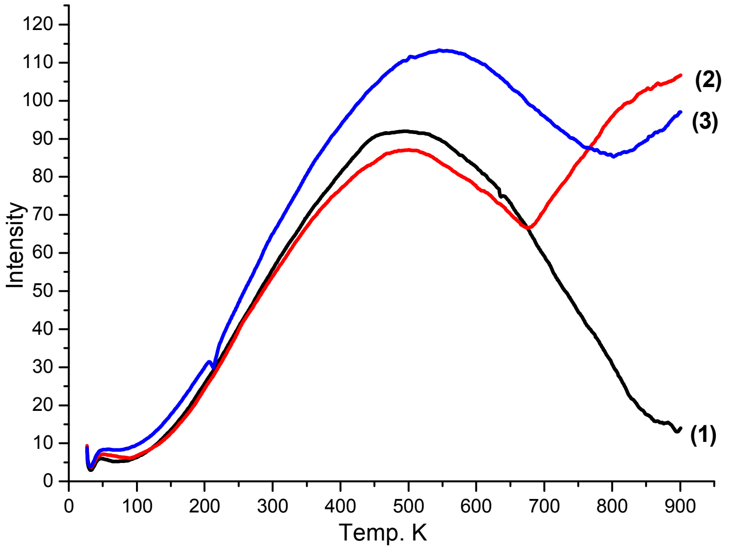

(b)

Fig. 5 (a) TGA & (b) DSC carves of prepared precursors (1), (2) and (3).

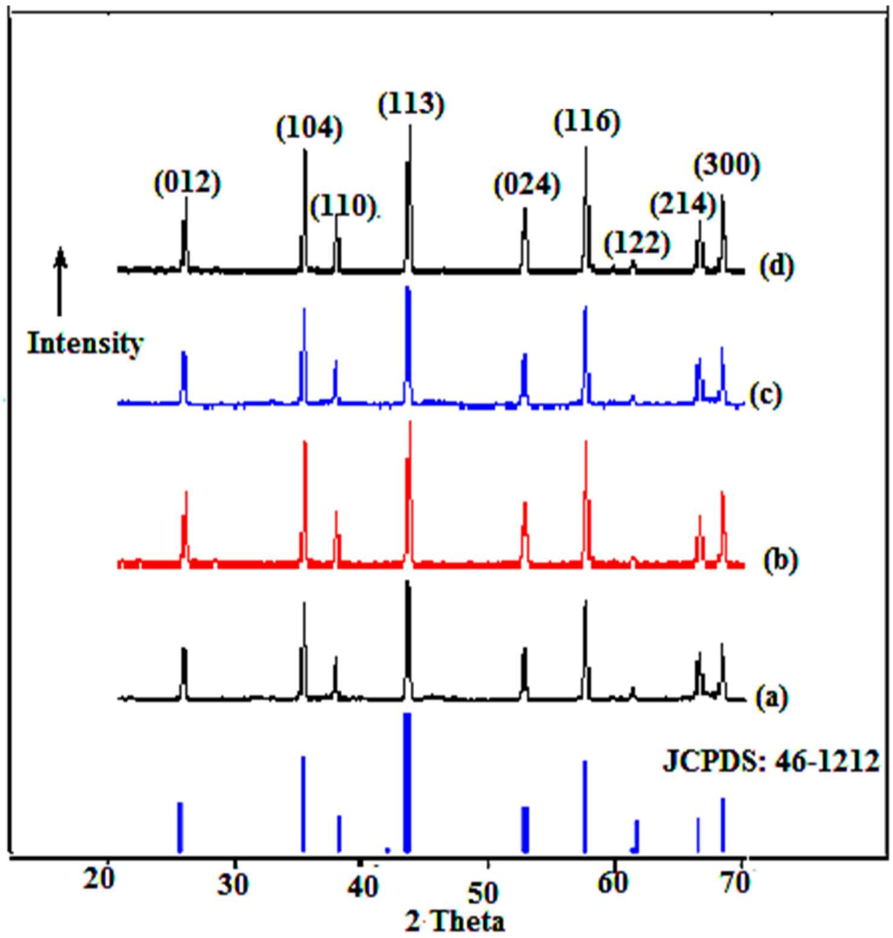

Fig.7 Combined XRD spectra of nano- crystalline α –Al_2O_3 (a) , (b) , (c) and (d) .

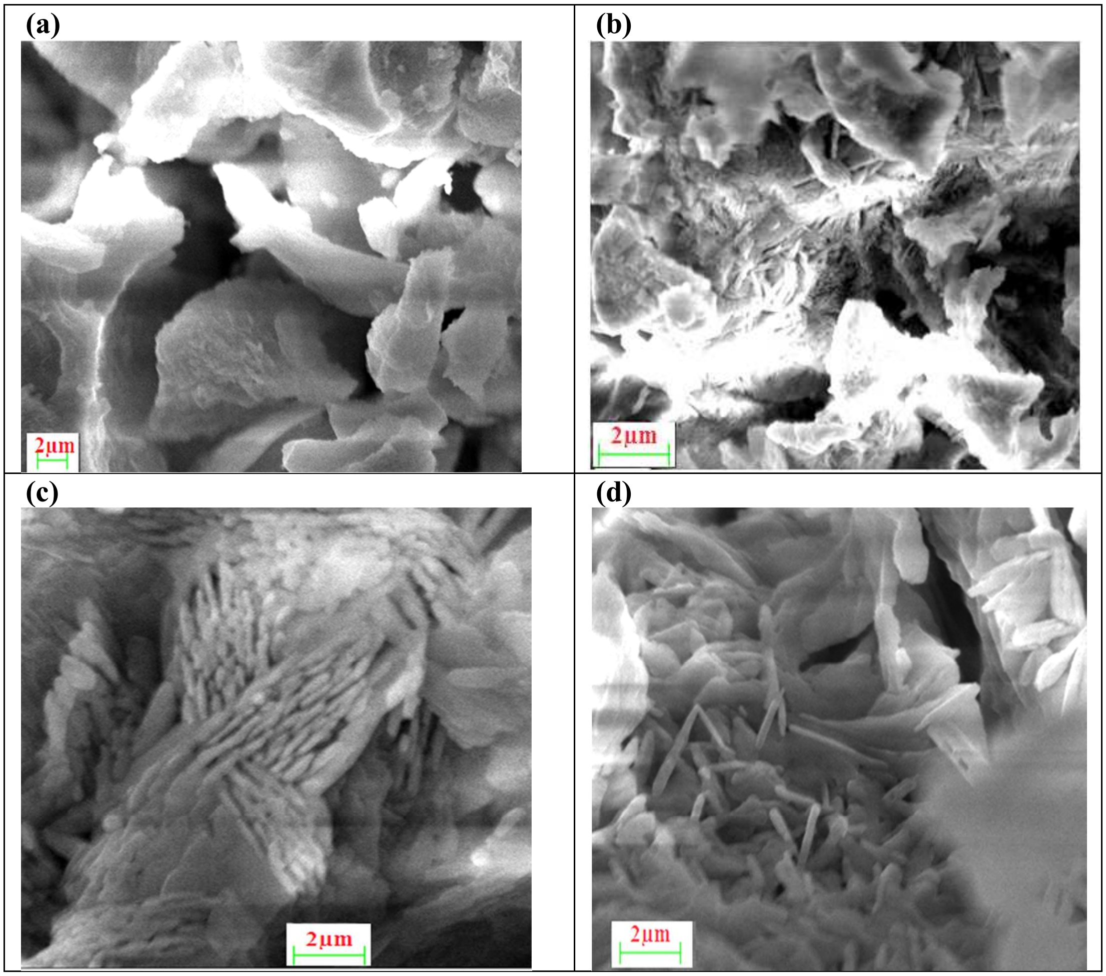

Fig.8 SEM images of nano- crystalline α –Al_2O_3, (a), (b), (c) and (d) .

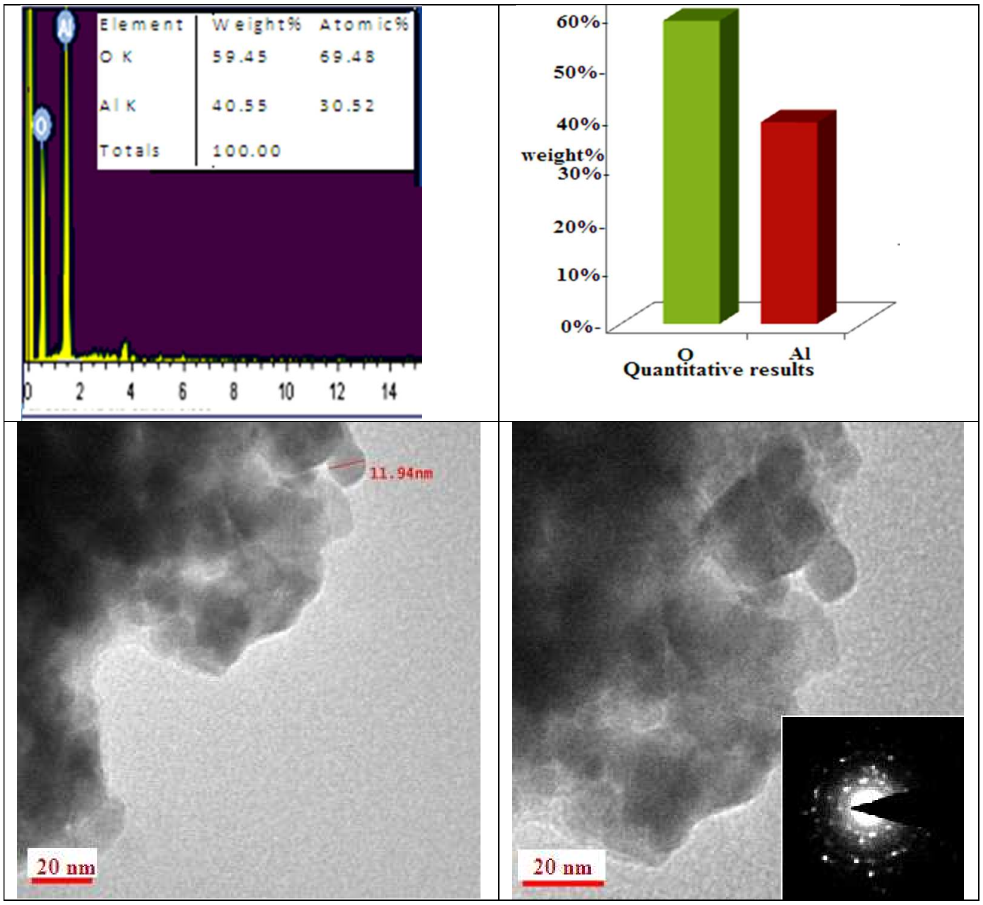

Element	Weight%	Atomic%
O K	59.45	69.48
Al K	40.55	30.52
Totals	100.00	

Fig.9 EDX , Quantitative weight % results and TEM images with corresponding SAED pattern of nano- crystalline α–Al_2O_3 (d).

Table-5 Crystal data and structure refinement for [Al($OC_6H_4CHO)_3$](3)

Complex	**[Al($OC_6H_4CHO)_3$](3)**
Empirical formula	$C_{21}H_{15}AlO_6$
Formula weight	390.31
Temperature (K)	150(2)
Wavelength (Å)	0.71073
Crystal system	Monoclinic
space group	P 2_1/n
Unit cell dimensions *a,* (Å) ,	9.5167(5),
b, (Å)	9.9644(3) ,
c, (Å)	19.0736(7)
α° ,	90,
β°	100.406(4) ,
γ°	90
Volume (Å^3)	1778.97(13)
Z	4
D_{calc} (mg/m^3)	1.457
Absorption coefficient (mm^{-1})	0.152
F(000)	808
Crystal size (mm^3)	0.33 x 0.26 x 0.21
θ range for data collection (°)	2.98 to 25.00
Limiting indices	-11<=h<=11, -11<=k<=11, -2<=l<=22
Reflections collected / unique	13807 / 3132
Independent reflections [$R_{(int)}$]	0.0962
Completeness to θ = 25.00	99.8 %
Absorption correction	Semi-empirical from equivalents
Maximum and minimum transmission	0.9688 and 0.9516
Refinement method	Full-matrix least-squares on F^2
Data / restraints / parameters	3132 / 0 / 253
Goodness-of-fit on F^2	1.015
Final R indices *[I>2σ(I)]*	R_1 = 0.0552, wR_2 = 0.1166
R indices (all data)	R_1 = 0.0857, wR_2 = 0.1340
Largest diffraction peak and hole (e. Å^{-3})	0.312 and -0.253

Table: 1 Synthetic and analytical data of Aluminium (III) isopropoxide derivetives (1 - 3)

C*	Reactants (a)= $Al(OPr^i)_3$, (b) = HOC_6H_4CHO	Nature of the Product	Mol .ratio	Yield % in g	Analysis % found (cal.) in g					
					Lib. Pr^iOH	OPr^i	Al	C	H	M.P ° C
(1)	(a)2.57g,12.58 mmol (b)1.54g,12.61mmol	Yellow solid	1:1	99.85	0.748g (0.75g)	0.11g (0.13)	10.0 (10.1)	58.52 (58.62)	7.10 7.13	~110
(2)	(a)2.81g, 13.75mmol (b)3.36g,27.51mmol	Yellow solid	1:2	99.76	1.63g (1.65g)	0.09 (0.10)	8.00 (8.21)	61.89 (62.14)	5.20 5.17	~150
(3)	(a)1.66g, 8.12 mmol (b)2.97g 24.34mmol	Yellow solid	1:3	99.86	1.44g (1.46g)	-	6.81 (6.88)	62.58 (64.35)	3.94 3.83	~189

Table: 2 Fragmented molecular ion m/e values of (1) to (3)

Complexes	Fragmented ions	m/e values
(3)	$[Al(OCHOC_6H_4)(OCHOC_6H_4) (OCHOC_6H_4)]^+$	389
	$[Al(OCHOC_6H_4) (OCHOC_6H_4)H_2]^+$	270
	$[Al(OCHOC_6H_4) (O2CH_5)H_2]^+$	198
	$[Al(OCHOC_6H_4) (OC)H2]^+$	177
	$[Al(OCHOC_6H_4) (O)H]^+$	164
	$[Al(OCHOC_6H_4)H]^+$	148
	$[Al(OCHC_4H_3)]^+$	106
	[Al(OC)]+	54
(2)	$[(OCHOC_6H_4)_2 Al(\mu\text{-}OC_3H_7)_2Al (OCHOC_6H_4)_2]^+$	655
	$[(OCHOC_6H_4)_2Al(\mu\text{-}OC_3H_7)_2Al (OCHOC_6H_4)]^+$	534
	$[(OCHOC_6H_4)_2Al(\mu\text{-}OC_3H_7)_2Al (OC_6H_5)]^+$	506
	$[(OCHOC_6H_4)_2Al(\mu\text{-}OC_3H_7)_2Al (OC_2H)]^+$	454
	$[(OCHOC_6H_4)_2Al(\mu\text{-}OC_3H_7)_2Al (O)]^+$	429
	$[(OCHOC_6H_4)Al(\mu\text{-}OC_3H_7)_2Al (O)]^+$	308
	$[(OC_6H_5)Al(\mu\text{-}OC_3H_7)_2Al (O)]^+$	379
	$[(OC_2H)Al(\mu\text{-}OC_3H_7)_2Al (O)]^+$	228
	$[(OH)Al(\mu\text{-}OC_3H_7)_2Al (O)]^+$	203
	$[(OH)Al(\mu\text{-}OC_3H_7)Al (O)]^+$	145
(1)	$[(OC_3H_7)_2Al(\mu\text{-}OC_3H_7)_2Al (OCHOC_6H_4)_2]^+$	531
	$[(OC_3H_7)_2Al(\mu\text{-}OC_3H_7)_2Al (OCHOC_6H_4)_2]^+$	410
	$[(OC_3H_7)_2Al(\mu\text{-}OC_3H_7)_2Al (OC_6H_5)]^+$	382
	$[(OC_3H_7)_2Al(\mu\text{-}OC_3H_7)_2Al (OC_2H)]^+$	330
	$[(OC_3H_7)_2Al(\mu\text{-}OC_3H_7)_2Al (O)]^+$	299
	$[(O_2C_3H_7) Al(\mu\text{-}OC_3H_7)_2Al (O)]^+$	256
	$[(O)_2Al(\mu\text{-}OC_3H_7)_2Al (O)]^+$	213
	$[(O)_2Al(\mu\text{-}OC_3H_7)Al (O)]^+$	176

Table: 3 FT-IR spectral data (cm^{-1}) and (^1H & ^{13}C NMR) spectral data (δ ppm) of (1),(2) and(3)

C*	**FT-IR spectral data**	**Isopropoxy**	**Salicylaldehyde moiety**					
	Compound	νC-O	νC-H	C=C	νAr-O	ν Al-O	νCHO	νAl-O-Al
(1)	$[Al(OPr^i)_2(OC_6H_4CHO)]_2$	1000s	3049w	1603s	1125m	643m	1660s	755w
(2)	$[Al(OPr^i)(OC_6H_4CHO)_2]_2$	1001s	3048w	1604s	1128m	645m	1650s	756w
(3)	$[Al(OC_6H_4CHO)_3]$	-	3047w	1605s	1131m	644m	1640s	-

C*	**^1H- NMR spectral data**				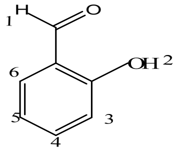
	Isopropoxy moiety		**Salicyladehyde moiety**		
	CH_3	-OCH<	CHO	OH	Aromatic protons
(1)	1.30-1.48,d(24H)	4.00-4.25(4H)sept	11.02,s(1H)	-	6.98 -7.58,m(4H)
(2)	1.11-1.33,d(12H)	4.05-4.29(2H)sept	11.01,s(2H)	-	6.98 -7.58,m(8H)
(3)	-	-	11.00 ,s(3H)	-	6.98 -7.58,m(12H)

C*	**^{13}C- NMR spectral data**				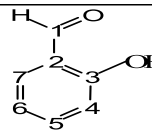
	Isopropoxy moiety		**Salicylaldehyde moiety**		
	CH_3	-OCH<	C1	C(3and 2)	Others C(4-7)
(1)	25.31-27.95	63.05-66.13	195.00	132.71-137.58	114.14-127.70
(2)	26.10-27.75	64.69-66.02	194.99	132.71-138.57	113.45-128.70
(3)	-	-	193.01	132.71-139.55	113.84-129.70

s = strong, m = medium, w = weak , C* = compound; s = singlet; d = doublet; m = multiplet; sept. = septet

Table 4. Selected bond lengths and bond angles in $[Al(OC_6H_4CHO)_3]$ (3)

Bond lengths *(A°)*

Al(1)-O(6)	1.836(2)	Al(1)-O(5)	1.914(2)
Al(1)-O(1)	1.841(2)	Al(1)-O(2)	1.936(2)
Al(1)-O(3)	1.846(2)	Al(1)-O(4)	1.947(3)
O(1)-C(1)	1.313(3)	O(4)-C(14)	1.267(4)
O(2)-C(7)	1.255(3)	O(5)-C(21)	1.261(4)
O(3)-C(8)	1.300(4)	O(6)-C(15)	1.323(3)
C(1)-C(2)	1.400(4)	C(1)-C(6)	1.434(4)
C(2)-C(3)	1.374(4)	C(4)-C(5)	1.349(4)
C(5)-C(6)	1.415(4)	C(3)-C(4)	1.396(4)
C(6)-C(7)	1.405(4)		

Bond angles *(°)*

O(6)-Al(1)-O(1)	94.53(11)	O(6)-Al(1)-O(3)	176.10(11)
O(1)-Al(1)-O(3)	88.89(10)	O(6)-Al(1)-O(5)	91.76(9)
O(1)-Al(1)-O(5)	92.07(10)	O(3)-Al(1)-O(5)	90.01(10)
O(6)-Al(1)-O(2)	88.25(9)	O(1)-Al(1)-O(2)	91.69(9)
O(3)-Al(1)-O(2)	89.76(9)	O(5)-Al(1)-O(2)	176.23(11)
O(6)-Al(1)-O(4)	87.52(10)	O(1)-Al(1)-O(4)	177.73(10)
O(3)-Al(1)-O(4)	89.03(10)	O(5)-Al(1)-O(4)	88.85(10)
O(2)-Al(1)-O(4)	87.39(9)	C(1)-O(1)-Al(1)	125.68(19)
C(7)-O(2)-Al(1)	122.23(18)	C(8)-O(3)-Al(1)	129.92(19)
C(14)-O(4)-Al(1)	127.1(2)	C(21)-O(5)-Al(1)	126.7(2)
C(15)-O(6)-Al(1)	129.74(19)	O(1)-C(1)-C(2)	121.3(3)
O(1)-C(1)-C(6)	121.5(3)	O(2)-C(7)-C(6)	126.9(3)
O(2)-C(7)-H(7)	116.5	O(3)-C(8)-C(9)	120.4(3)
O(3)-C(8)-C(13)	122.8(3)	O(4)-C(14)-C(13)	125.9(3)
O(4)-C(14)-H(14)	117.0	O(5)-C(21)-C(20)	126.5(3)
O(5)-C(21)-H(21)	116.7	O(6)-C(15)-C(16)	119.9(3)